

EFFECT OF THE Mg SUBSTITUTION ON THE STRUCTURAL, OPTICAL AND ELECTRICAL PROPERTIES OF CuCrO₂ FOR APPLICATIONS TO P-TYPE DYE-SENSITIZED SOLAR CELLS

Ursu DANIEL^{1,2}, Miclău MARINELA², Bănică RADU^{1,2}, Bucur RAUL², Vaszilcsin NICOLAE¹, Chiosa MONICA¹

¹ Politehnica University of Timisoara, Timisoara, Romania, EU, rector@rectorat.upt.ro

² National Institute for Research and Development in Electrochemistry and Condensed Matter, Timisoara, Romania, EU

Abstract

Delafossite CuCrO₂ is an important p-type semiconductor used in dye-sensitized solar cells (p-DSSCs) due to its potential role in the elaboration of future dual dye solar cells with a photoanode and a photocathode built upon n-type respectively p-type semiconductors,. In the present study, we report electrical and optical properties of Mg substitution CuCrO₂, obtained by hydrothermal method using Cu₂O, Cr(OH)₃ and MgO as precursors. The crystal structure of CuCr_{1-x}Mg_xO₂, where (x = 0 ÷ 0.05), was investigated by X-ray diffraction. A shift of the diffraction peak belonging to the crystallographic plane (1 1 0) has been observed, caused by the distortion of the lattice, due to M ionic radius increasing CuMO₂, in according with the difference between Mg²⁺ radii (r = 0.66 Å) and Cr³⁺ radii (r = 0.63 Å). From scanning electron micrographs it can be observed seen that the nanometric size of the particles is about 20 - 50 nm. EDX measurements confirm the purity of the material where only Cu, Cr and Mg characteristic peaks are present. Optical characterization reveals that the band gap energy of the CuCr_{1-x}Mg_xO₂ increases with increasing of Mg²⁺ concentration, from 2.86 eV (x= 0) to 2.91 eV (x= 0.05). Thus, Mg-doped CuCrO₂ may have potential applications for p-type dye-sensitized solar cells.

Keywords: Nanocrystal, Delafossite, Hydrothermal, Dye-Sensitized Solar Cell

INTRODUCTION

In recent years, delafossite-type oxides CuMO₂ have received considerable attention as promising candidates for a thermoelectric material [1-2], dye-sensitized solar cells [3-4], touch screens, gas sensors, light-emitting diodes, etc [5]. Delafossite structure materials are considered transparent conducting oxides (TCOs) because they are unique materials that combine simultaneously high electrical conductivity and optical transparency in a single material [6]. In the delafossite structure, each Cu atom is linearly coordinated with two oxygen atoms, forming O–Cu–O dumbbells parallel to the c axis. The M cation is located central in distorted edge-shared MO₆ octahedra [7]. Depending on the orientation of each layer in stacking, two crystalline forms can exist, namely rhombohedral (3R), and hexagonal (2H) [8]. According to the literature, delafossite structure doping with different materials leads to increased electrical and optical properties. Thereby, the Mg²⁺ doped CuCrO₂ was obtained using different methods such as: solid-state reaction [9], pulsed laser deposition [10], sol-gel [11] and hydrothermal procedures [12]. However, in spite of a wide range of applications, these materials present some drawbacks including relatively low conductivities, low carrier mobilities [13]. Doping the trivalent metal site (A⁺¹B⁺³O₂) in the delafossite structure with a divalent dopant is well known. Increasing the mobility of holes in p -type delafossites will lead to increased Cu d orbital overlap. The lower hole mobilities in p -type delafossites relative to Cu₂O may be caused by the lack of Cu–O–Cu linkages [14]. In this paper we present the partial substitution of Cr by Mg and characterization of CuCr_{1-x}Mg_xO₂ where (x = 0 ÷ 0.05) obtained by hydrothermal method.

1. EXPERIMENTAL

Polycrystalline samples with compositions $\text{CuCr}_{1-x}\text{Mg}_x\text{O}_2$ where ($x = 0, 0.03, 0.05$) was synthesized by hydrothermal method. The stoichiometric mixture of 1 mmol Cu_2O , $(2 - x)$ mmol $\text{Cr}(\text{OH})_3$ [15] was mixed with 42 ml distilled water. NaOH was used to control metal oxide solubility and oxidation state of Cu, respectively. The chemicals were purchased from Sigma Aldrich and had a high degree of purity (>99.99 %). The obtained solution was transferred in a teflon lined autoclave, with a filling degree of 70%. The autoclave was heated at 250 C for 60 hours. After that, the autoclave was cooled down to room temperature naturally. The precipitate was filtered and washed with deionized water and stirring with liquid ammonia (30 %) and distilled water to remove any Cu_2O impurity to obtain phase pure $\text{CuCr}_{1-x}\text{Mg}_x\text{O}_2$ where ($x = 0 \div 0.05$). The product was dried in an oven at 80 °C for 4 h. The structure of products was determined by powder X-ray diffraction (XRD) PW 3040/60 X'Pert PRO using Cu-K α radiation with $\lambda=1.5418$ Å, in the range $2\theta = 10 - 80^\circ$. A Scanning Electron Microscope Inspect S (SEM) was used to observe the morphology of synthesized nanocrystals. The diffuse reflectance spectra (DSR) was obtained using a Lambda 950 UV-Vis-NIR Spectrophotometer with 150 mm integrating sphere in the wavelength range of 300–800 nm. All the measurements were performed at room temperature. The electrical resistivity was measured on a cylindrical bar with a diameter of 7.2 mm and height of 1.5 mm using Digit Precision Multimeter HM8112-3 Hameg Instruments in temperature ranging from 300– 430 K with good ohmic contacts.

2. RESULTS AND ITS DISCUSSION

Fig. 1 shows the XRD patterns for $\text{CuCr}_{1-x}\text{Mg}_x\text{O}_2$ where ($x = 0 \div 0.05$) compound, obtained by hydrothermal method. As can be seen from XRD patterns, all the samples are single-phase delafossite (space group R-3m), with no secondary phase present such as Mg (JCPDS card 00-04-0770) [16], MgO (JCPDS card 01-087-0651) [17] or CuO (JCPDS card 00-48-1548) [18]. Also, for Mg^{2+} substituted CuCrO_2 , the peak (1 1 0) has a visible shift due the difference between ionic radius of Mg^{2+} radii ($r = 0.66$ Å) and Cr^{3+} radii ($r = 0.63$ Å). [19].

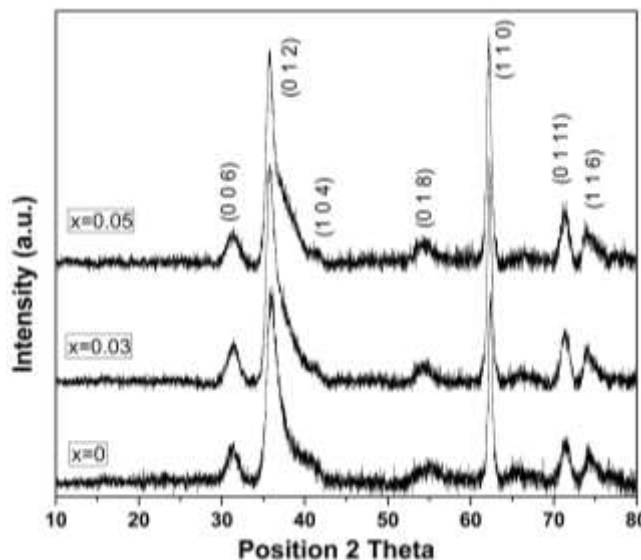


Fig. 1. X-ray diffraction patterns of $\text{CuCr}_{1-x}\text{Mg}_x\text{O}_2$ ($x = 0 \div 0.05$)

The average crystallite size was calculated from line broadening of the crystallographic plane (0 1 2) using Scherrer's equation (1) [20].

$$D_{hkl} = \frac{k\lambda}{B \cos \theta} \quad (1)$$

where k is a constant (~ 1), B is the full width at half maximum (FWHM), λ is the wavelength of x-ray and θ is the diffraction angle. The average crystallite size increases with Mg^{2+} content from 25 nm for $x=0$ to 45 nm for $x=0.05$. The morphology of the compound $CuCr_{1-x}Mg_xO_2$ was observed by scanning electron micrography at high resolution as shown in Fig. 2. From SEM image, it is obvious that the product consists of agglomerations with size distribution varying from 10 to 80 nm. Semi-quantitative EDX analysis for $CuCr_{1-x}Mg_xO_2$ ($x = 0$) sample confirmed the composition with the precursor material $Cu : Cr = 49 : 50$ and for $CuCr_{1-x}Mg_xO_2$ ($x = 0.05$), no impurity trace was found, only the Cu, Cr and Mg elements. Magnesium presence in the sample was highlighted by K-line located at 1.2 keV.

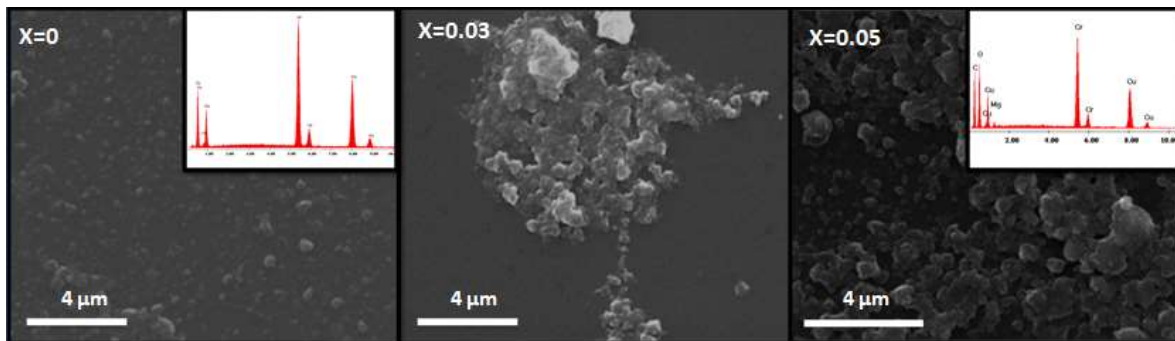


Fig. 2. SEM image of $CuCr_{1-x}Mg_xO_2$ ($x = 0 \div 0.05$) and inset with EDX analysis

The optical bandgap (E_g) of $CuCr_{1-x}Mg_xO_2$ are calculated from the diffuse reflectance spectra in the wavelength of 300–800 nm, using the $[(k/s)hv]^2$ vs. hv plots, where hv is the photon energy; k and s denote the absorption and scattering coefficients respectively. The ratio (k/s) can be calculated from the diffuse reflectance spectra using the Kubelka–Munk equation [21, 22]. The $[(k/s)hv]^2$ vs. hv plots of $CuCr_{1-x}Mg_xO_2$ where ($x = 0 \div 0.05$) is shown in Fig. 3, where the bandgap are found to be 2.86 eV for $x = 0$, and 2.91 eV for $x = 0.05$. The value of band gap for pure $CuCrO_2$ is closed to that reported in literature [23]. A gradual increase of E_g is observed with the Mg content. This result confirms that the $CuCr_{1-x}Mg_xO_2$ where ($x = 0 \div 0.05$) are direct energy gap above 2.91 eV that is suitable for applications such as TCO materials and p-type dye-sensitized solar cells.

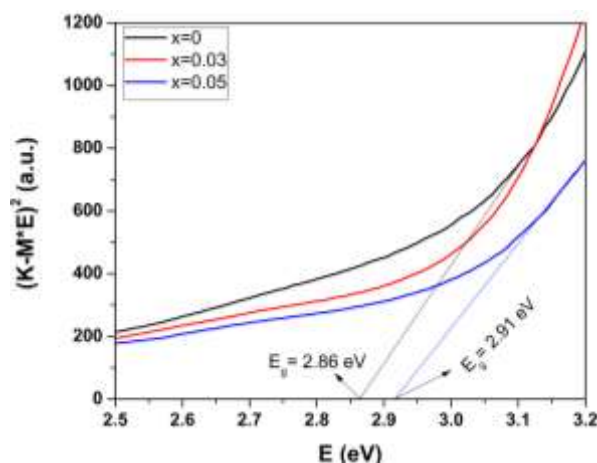


Fig. 3. Optical band gaps of the $CuCr_{1-x}Mg_xO_2$ ($x = 0 \div 0.05$) nanocrystals

According to the literature, undoped $CuCrO_2$ is a semi-conductor with a high resistivity, however, substitution of divalent dopants such as Mg, Mn, Ni for trivalent Cr in this system leads to a marked increase in conductivity [24, 25]. T. Okuda et al. showed that the increase in conductivity is linked to Cu^I/Cu^{II} [2, 26] and to Cr^{III}/Cr^{IV} hole mechanisms [27]. The temperature dependence of the electrical resistivity $CuCr_{1-x}Mg_xO_2$

where ($x = 0 \div 0.05$) is shown in Fig. 4. The electrical resistivity decreases with increasing temperature ($d\rho/dT < 0$), indicating a semiconductor behavior. At room temperature the resistivity decreases sequentially with increasing Mg^{2+} content from $\rho = 0.14 \cdot 10^3$ ($\Omega \text{ cm}$) for ($x=0$) to $\rho = 0.04 \cdot 10^3$ ($\Omega \text{ cm}$) for ($x = 0.05$).

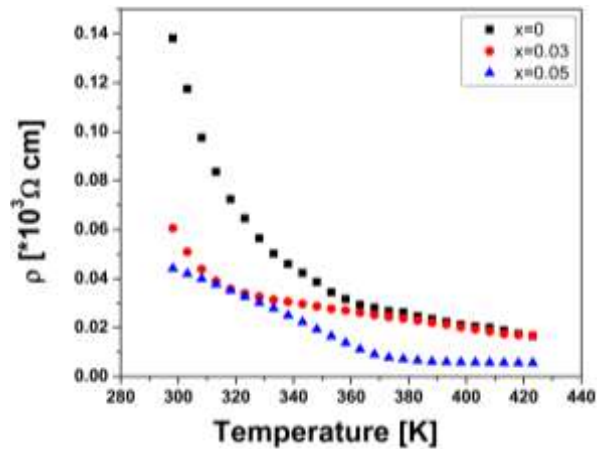


Fig. 4. Temperature dependence of the electrical resistivity in the series $CuCr_{1-x}Mg_xO_2$ ($x = 0 \div 0.05$) nanocrystal

For semiconductor, the electrical resistivity is described by the relation of $\rho = A \exp(E_a/k_B T)$ [28, 29] where E_a is the activation energy which is minimum energy to product carrier from the top edge valence band level to the acceptor level, k_B is the Boltzmann's constant, T is the temperature and A is the constant. The value of E_a is shown in Fig. 5 and is obtained from the Arrhenius plot by linear curve of $\ln(\rho)$ as a function of $1/T$. The activation energy (E_a) of the $CuCr_{1-x}Mg_xO_2$ ($0 \leq x \leq 0.05$) samples is $E_a = 247$ meV ($x = 0$), $E_a = 157$ meV ($x = 0.03$) and $E_a = 112$ meV ($x = 0.05$). The activation energy is the energetic difference from an acceptor level to the valence band maximum (VBM) for p-type semiconductors or from the conduction band minimum (CBM) to donor level for n-type semiconductors [30].

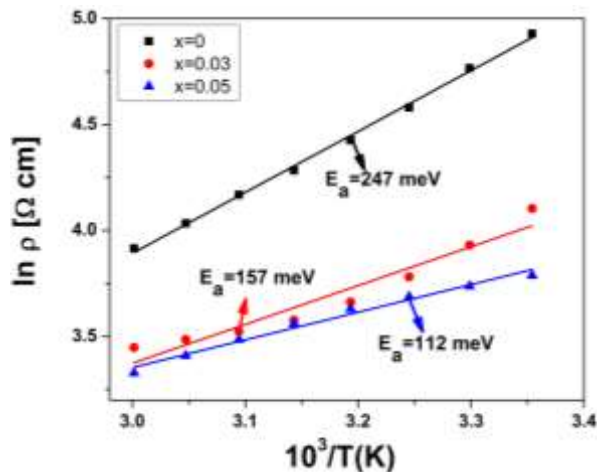


Fig. 5. Plots of $\ln \rho$ vs. $10^3/T$ of the $CuCr_{1-x}Mg_xO_2$ where ($x = 0, 0.03, 0.05$). The linear fit of each curve determines the activation energy E_a of each sample.

CONCLUSION

The electrical and optical properties of Mg^{2+} substituted $CuCrO_2$, obtained by hydrothermal method were investigated. From XRD results show that with increasing Mg^{2+} content the (1 1 0) peak, has a shift, which prove incorporating of this metal in $CuCrO_2$ structure. From SEM images, nanometer sized particles is observed and from EDX analysis for $CuCr_{1-x}Mg_xO_2$ ($x = 0$) sample confirmed the closely stoichiometric composition with the precursor material $Cu : Cr = 49 : 50$ and for $CuCr_{1-x}Mg_xO_2$ ($x = 0.05$), no impurity trace not found, only the Cu, Cr and Mg elements The optical band gap, determined by DSR spectra, is increasing

from 2.86 eV to 2.91 eV with the rise from $x = 0$ to $x = 0.05$ of Mg^{2+} content in $\text{CuCr}_{1-x}\text{Mg}_x\text{O}_2$. The electrical resistivity decreases with increasing temperature due to the increase of the Mg content from $\rho = 0.14 \cdot 10^3$ ($\Omega \text{ cm}$) for ($x=0$) to $\rho = 0.04 \cdot 10^3$ ($\Omega \text{ cm}$) for ($x = 0.05$) indicating semiconductor behavior. From this results it has been shown that, $\text{CuCr}_{1-x}\text{Mg}_x\text{O}_2$ nanocrystals will be considered as one of promising candidates for p-type dye-sensitized solar cell if the conductivity will be improved.

ACKNOWLEDGEMENTS

This paper is supported by the Sectoral Operational Programme Human Resources Development (SOP HRD), financed from the European Social Fund and by the Romanian Government under the project number POSDRU/159/1.5/S/134378.

REFERENCES

- [1] ISAWA, K. YAEGASHI Y., OGOA S., NAGANO M., SUDO S., YAMADA K., and YAMAUCHI H., Phys. Rev. B , 1998, 57, pp. 7950-7954.
- [2] OKUDA, T., JUFUKU, N., HIDAHA, S., and Terada, N.: Phys. Rev., 2005, B 72, 144403
- [3] NATTESTAD, A., ZHANG, X., BACH, U. and CHENG, Y. B., J. Photonics Energy, 2011, 1, 011103.
- [4] YU, M. Z., NATU, G., JI, Z. Q. and WU, Y. Y., J. Phys. Chem. Lett., 3, 2012, 1074.
- [5] THU, T. V., THANH, P. D., SUEKUNI, K., HAI, N. H., MOTT, D., KOYANO, M., MAENOSONO, S. Mater. Res. Bull.. 2011, 46, 1819–1827.
- [6] GORDON, R. G. MRS Bull. 2000, 25, 52–57
- [7] MARQUARD, M , ASHMORE, N, CANN D, Thin Solid Films, 2006, 496, 146 – 156
- [8] MICLAU, M., URSU D., KUMAR, S., GROZESCU, I., J Nanopart Res 2012 141110
- [9] HAYASHI, K., SATO, K., NOZAKI, T., and KAJITANI. T., Japanese Journal of Applied Physics, 2008, 47, 1, pp. 59–63
- [10] SADIK P.W., IVILL M., CRACIUN V., D.P. Norton, Thin Solid Films, 2009, 517, 3211–3215
- [11] WANG, Y. , GU, Y. , WANG, T. , SHI, W. , Journal of Alloys and Compounds, 2011, 509, 19, pp.5897–5902
- [12] XIONG, D., ZHANG, W., ZENG, X., XU, Z., CHEN, W., CUI, J., WANG. M., SUN, L., CHENG, Y.B., Chem Sus Chem. 2013, 6, 8, pp. 1432-7
- [13] VARADARAJAN, V., Norton, D. P., Appl. Phys. A: Mater. Sci. Process., 2006, 85, 117
- [14] NAGARAJAN, R., DUAN, N., JAYARAJ, M. K., LI, J., VANAJA, K. A., YOKOCHI, A., DRAESEKE A., TATE, J. and SLEIGHT, A. W., Int. J. Inorg. Mater., 2001,3 , 265–270
- [15] MICLAU, M., URSU, D., KUMAR, S., GROZESCU, I., 2012, J Nanopart Res, 14:1110
- [16] SWANSON and TAGE, JC Fe. Reports, NBS., Natl. Bur. Stand. Report, 1951
- [17] BROCH, E., Z. Phys. Chem. Neue Folge. (Wiesbaden), 1927, 127, 446
- [18] DIAZ-GUERRA, C., VILA, M., PIQUERAS, J., Appl. Phys. Lett., 2010, 96, 193105
- [19] SHANNON, R. D., ROGERS, D. B., PREWITT, C. T., Inorganic Chemistry, 1971,10 , 713
- [20] BAGHERI, M., SHOKOOH, S. M., Semicond. Sci. Technol., 2004, 19, 764-769
- [21] KUBELKA, P., MUNK, F., Zh. Tekh. Fiz., 1931, 12, 593.
- [22] KUBELKA, P., J. Opt. Soc. Am. 1948, 38, 448
- [23] ZHOU, S., FANG, X., Journal of Crystal Growth, 2008, 310, 5375–5379
- [24] LUO, S., WANG, K. F., LI, S. Z., DONG, X. W., YAN, Z. B., CAI, H. L. and LIU, J., Appl. Phys. Lett. , 2009, 94 , 172504
- [25] LUO, S., LI, L., WANG, K. F., LI, S. Z., DONG, X. W., YAN, Z. B. and LIU, J., Thin Solid Films , 2010, 518 , 50–53
- [26] OKUDA, T., BEPPU, Y., ONOE, T., TERADA, N., MIYASAKA, S., Phys Rev. B , 2005, 77 , 134423.
- [27] ONO, Y., SATOH, K., NOZAKI, T., KAJITANI, T., Jpn. J. Appl. Phys., 2007,46, 1071–1075.

- [28] COX, P. A., Transition Metal Oxides an Introduction to Their Electrical Structure and Properties. Clarendon Press, Oxford, 1995
- [29] KO, D., URBAN, J. J., MURRAY, C.B., J. Nano Lett., 2010, 10, 1842-1847
- [30] JIANGA, H. F., ZHUA, X. B., LEI, H. C. , LI, G., YANG, Z. R., SONGA, W. H., DAI, J. M., SUNA, Y.P., FUC, Y.K, Journal of Alloys and Compounds, 2011, 509, 1768–177.